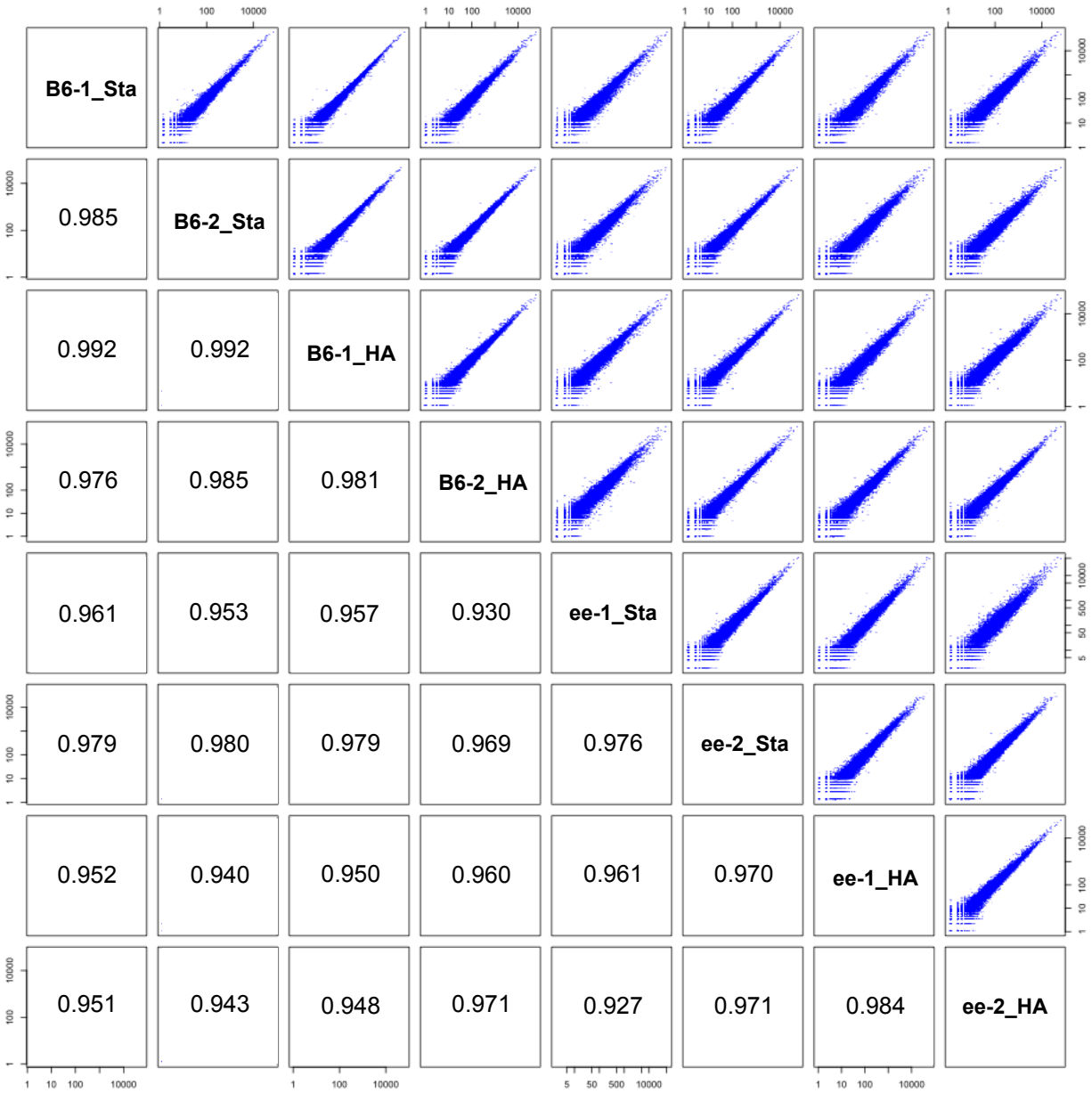

Supplementary Figure 1. Technical replicates of mouse EDGE libraries.
EDGE libraries from *Mc1r*$^{+/+}$ (B6-1 and B6-2) and *Mc1r*$^{e/e}$ (ee-1 and ee-2) were constructed from adult mouse skin. Each library was sequenced at two different locations, Stanford University (Sta) and HudsonAlpha Institute for Biotechnology (HA). Pairwise scatter plots comparing normalized gene counts are plotted on a $\log_{10}$ scale above the diagonal. Pearson correlation coefficients are shown below the diagonal.

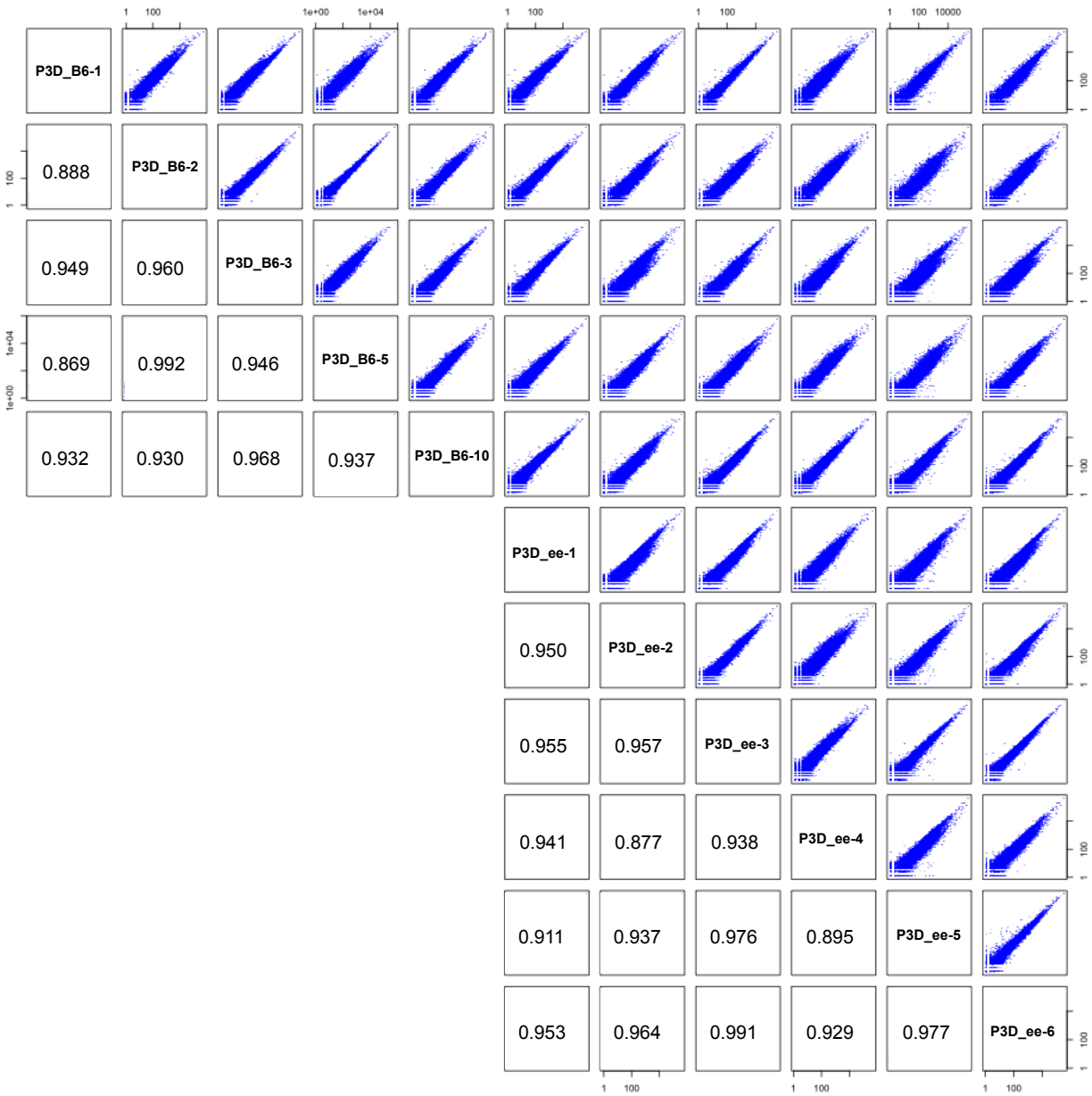

Supplementary Figure 2A. Biological replicates of mouse EDGE libraries from neonate dermis. Pairwise scatter plots comparing normalized gene counts between *Mc1r*$^{+/+}$ (B6) and *Mc1r*$^{e/e}$ (ee) EDGE libraries are plotted on a $\log_{10}$ scale above the diagonal. Pearson correlation coefficients are shown below the diagonal.

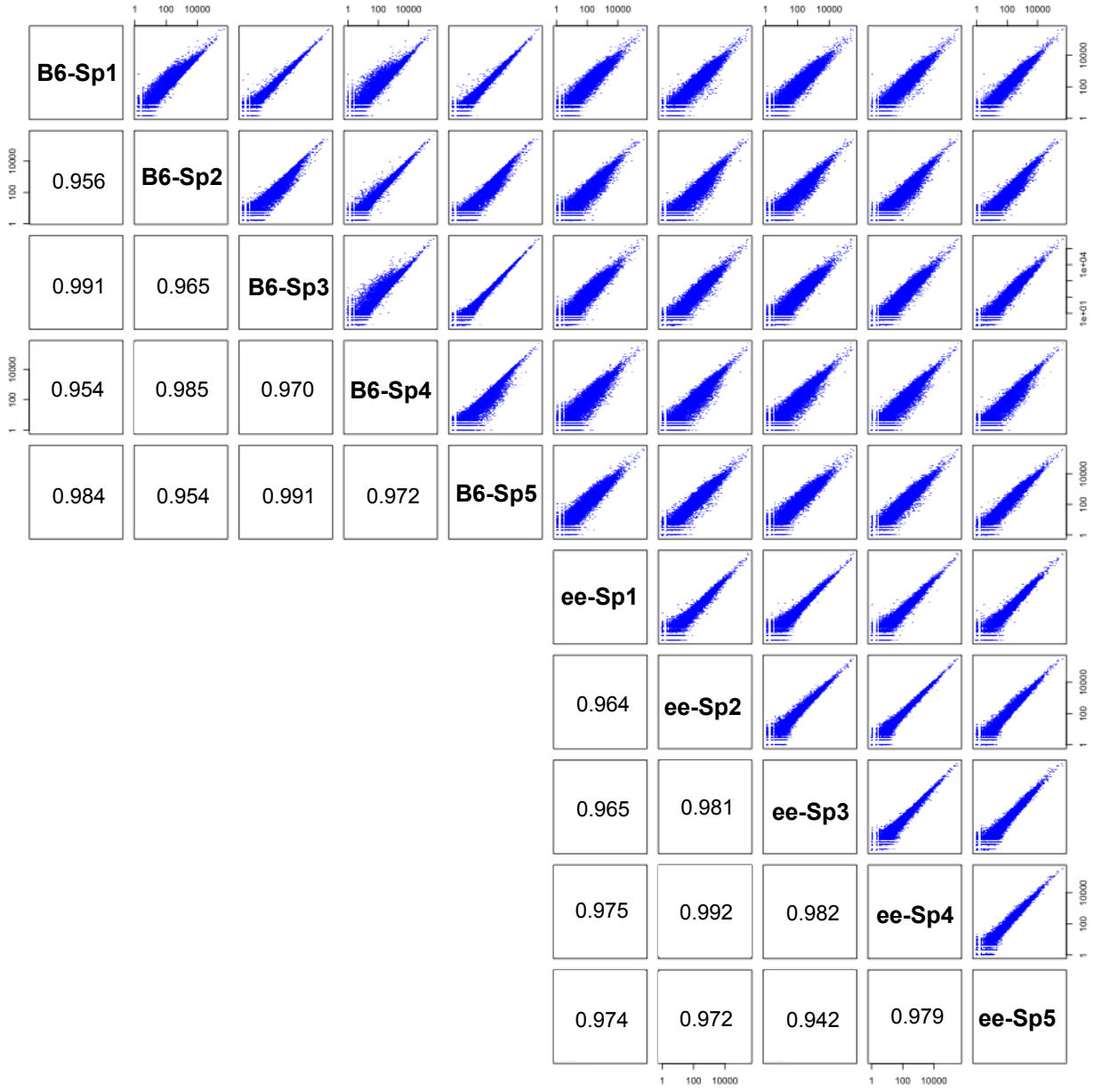

Supplementary Figure 2B. Biological replicates of mouse EDGE libraries from spleen
Pairwise scatter plots comparing normalized gene counts between *Mc1r*$^{+/+}$ (B6) and *Mc1r*$^{e/e}$ (ee) EDGE libraries are plotted on a $\log_{10}$ scale above the diagonal. Pearson correlation coefficients are shown below the diagonal.

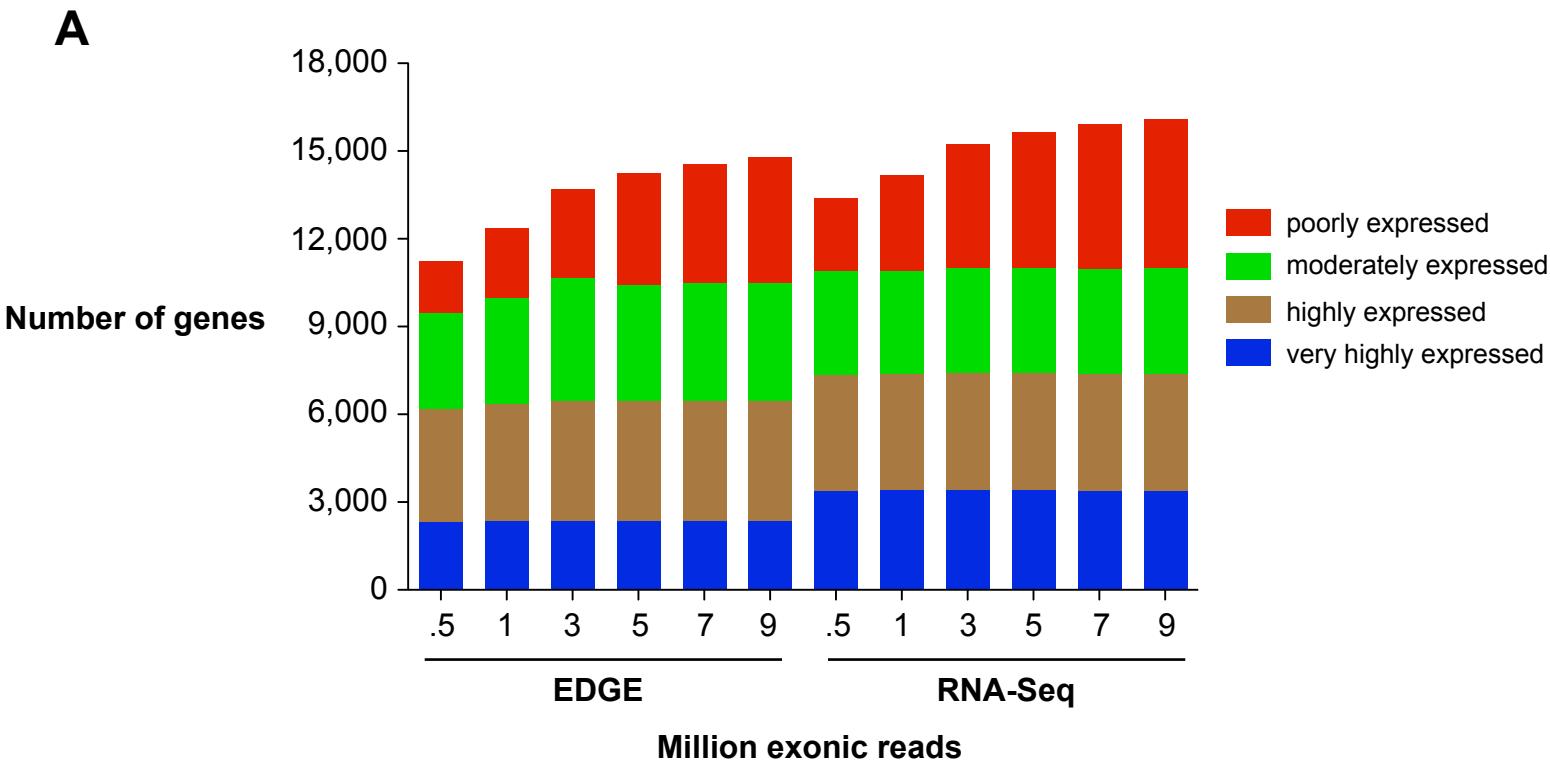

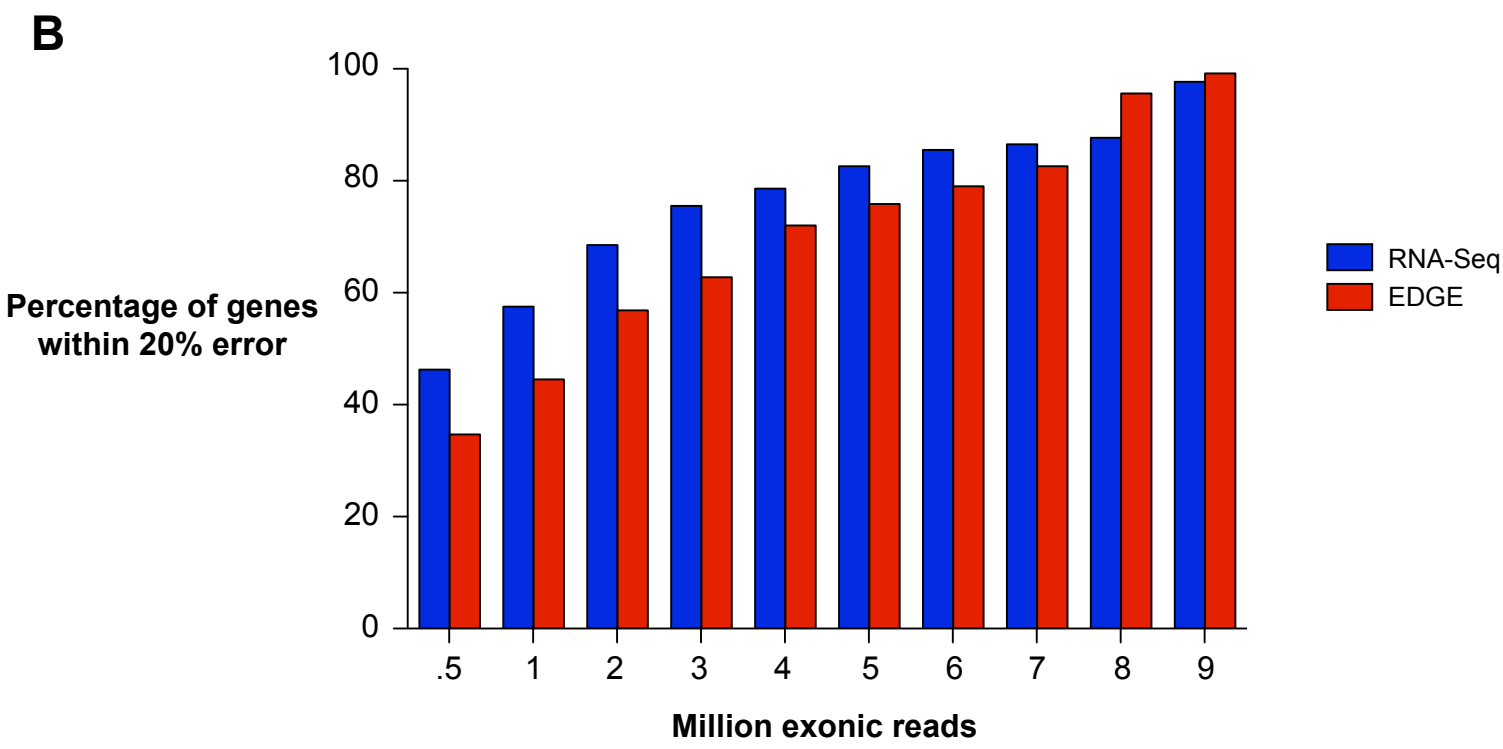

Supplementary Figure 3. Sequencing depth analysis.
EDGE and RNA-Seq libraries generated from a mouse neonatal dermis sample (each sequenced on one lane of the Illumina GAIIx) were aligned to mouse RefSeq transcripts and the following characteristics were determined as a function of increasing sequencing depth:
(A) number of genes within each expresion category (poorly expressed: <2 TPM or <1.5 RPKM, moderately expressed: 2 to 10 TPM or 1.5 to 5 RPKM, highly expressed: 10 to 50 TPM or 5 to 15 TPM, very highly expressed: > 50 TPM or >15 RPKM).
(B) percentage of genes with TPM or RPKM values within 20% of the value for that gene in the total dataset.

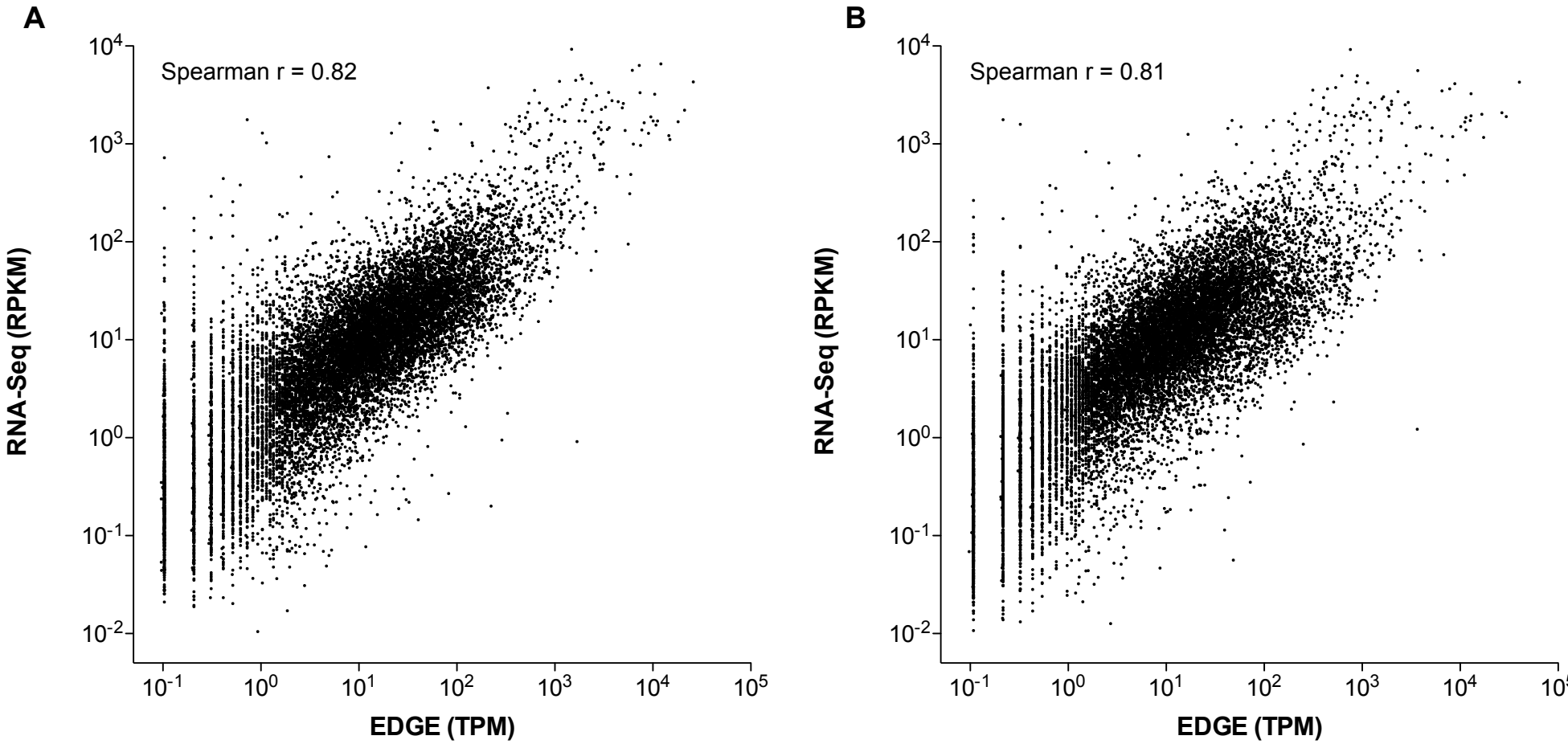

Supplementary Figure 4. RNA-Seq and EDGE provide similar assessments of relative transcript abundance.
Relative transcript levels measured by RNA-Seq and EDGE were compared by plotting RPKM and TPM for each gene in (A) *Mc1r*$^{+/+}$ (Spearman r = 0.82) and (B) *Mc1r*$^{e/e}$ (Spearman r = 0.81) from mouse neonate dermis. Each point reflects the RPKM and TPM value from a single RNA-Seq and EDGE library.

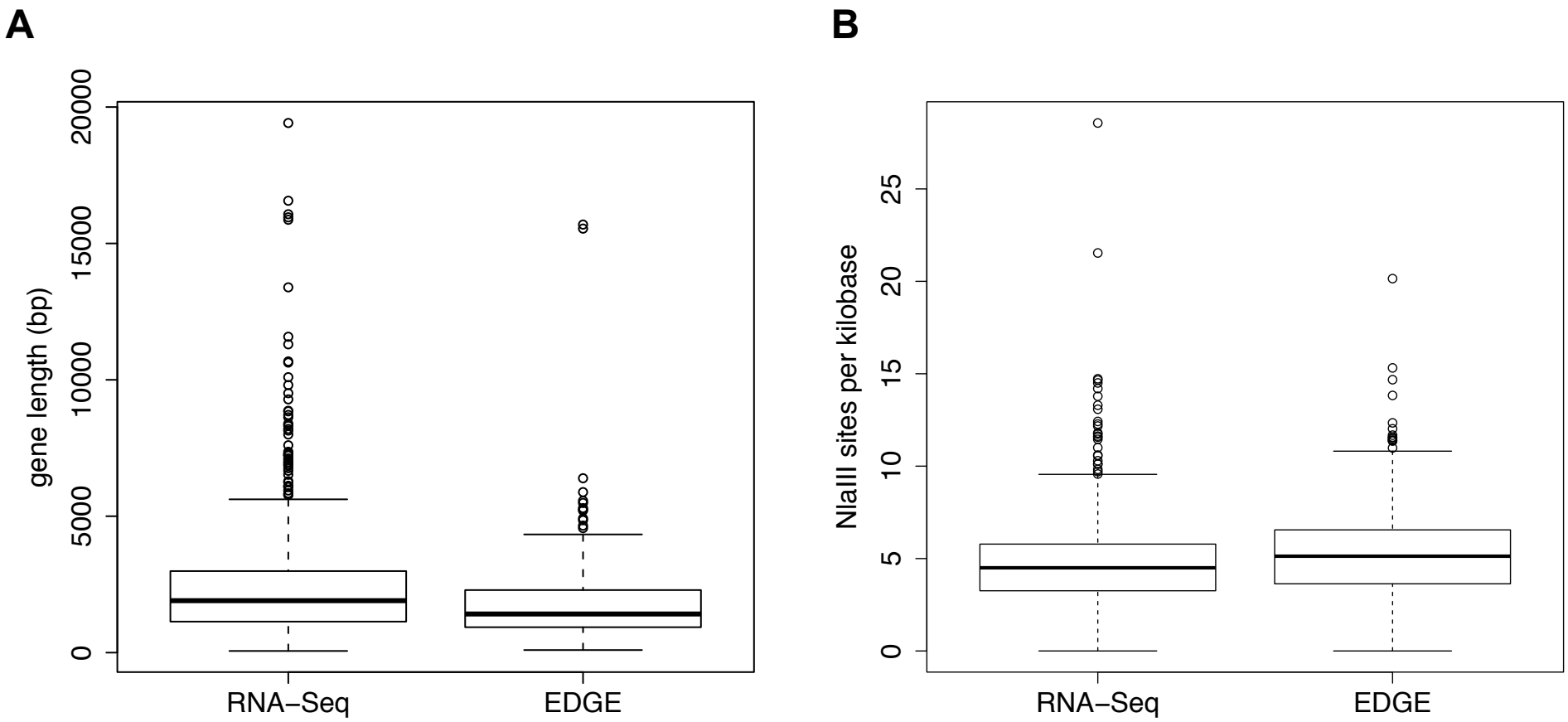

Supplementary Figure 5. Transcript length and *NlaIII* site frequency.
The 436 genes detected only by EDGE and 1,295 genes detected only by RNA-Seq were characterized for (A) transcript length and (B) frequency of *NlaIII* sites. (A) The average length of genes detected only by EDGE is 548 bp shorter than the genes detected only by RNA-Seq ($p < 1e-8$). (B) Genes that were only detected by EDGE and genes that are only detected by RNA-Seq have 5.4 and 4.6 *NlaIII* sites per kilobase of transcript, respectively ($p < 1e-6$).

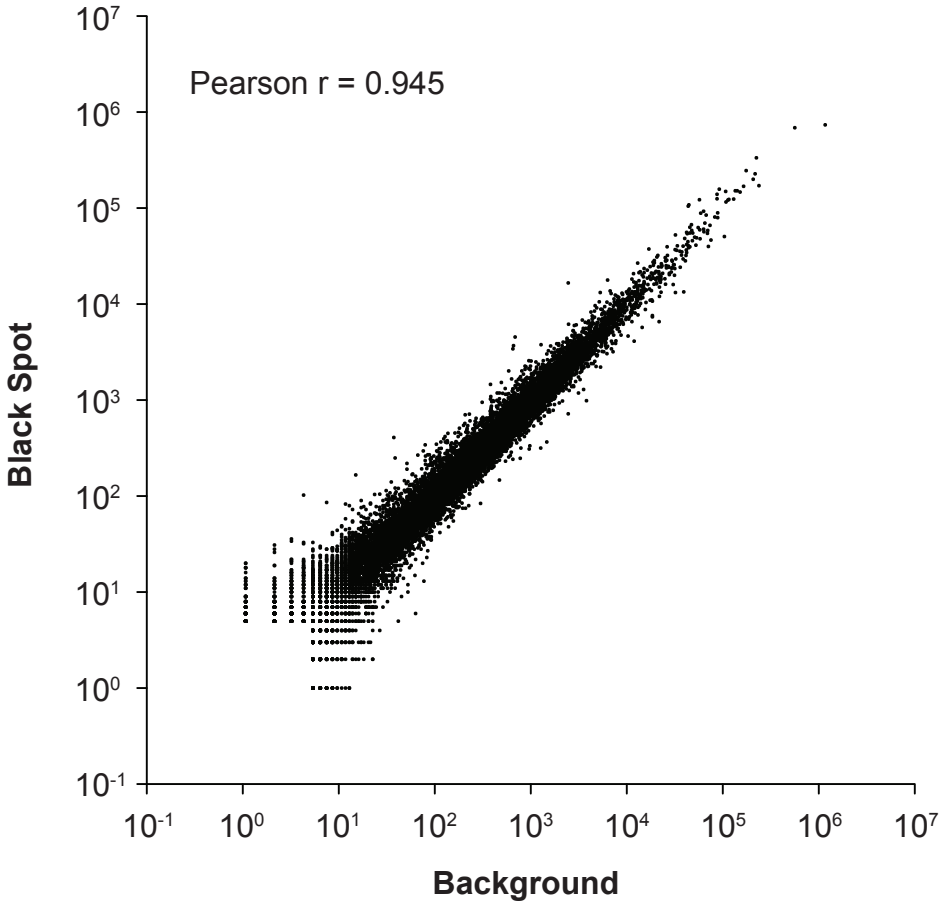

Supplementary Figure 6. EDGE in cheetah skin.
Normalized expression of 14,247 genes from the black spot and yellow background regions of cheetah skin was measured by EDGE and plotted on a $\log_{10}$ scale. The two libraries are highly correlated (Pearson r = 0.945).

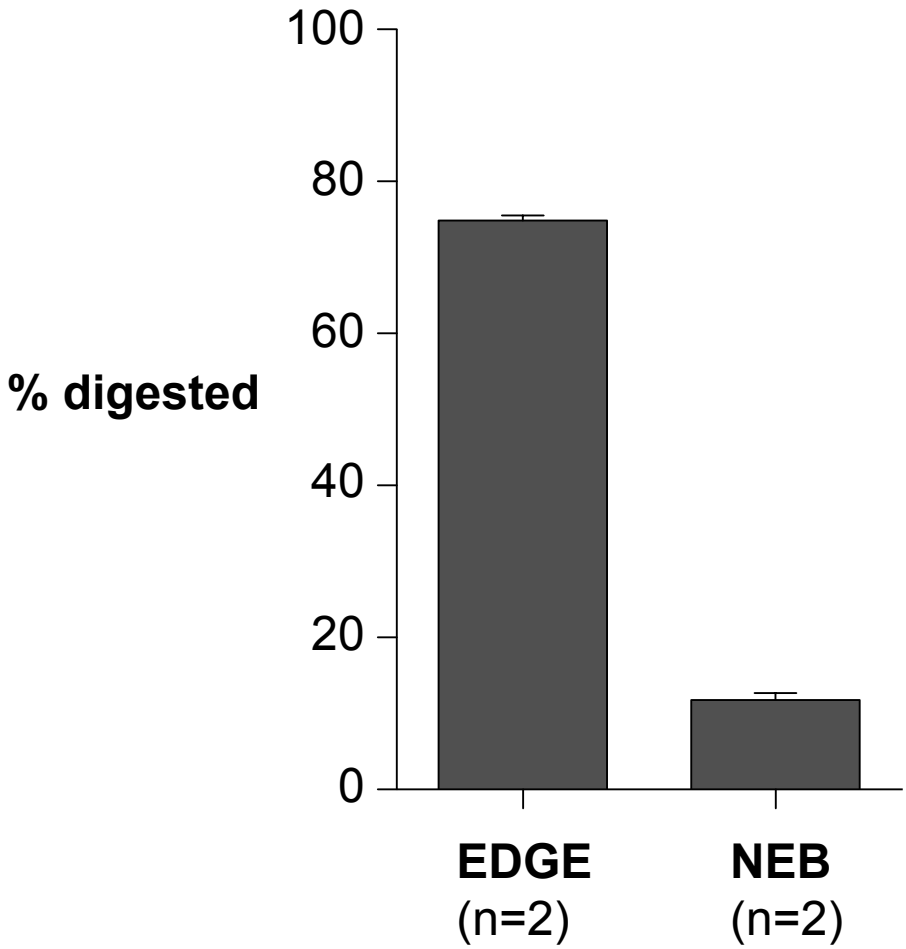

Supplementary Figure 7. *EcoP15I* cleavage efficiency.
DNA template carrying a single *EcoP15I* recognition site was generated by PCR and subjected to restriction digest with *EcoP15I* for 16 hours at 37°C. Duplicate reactions were set up according to the reaction conditions in the EDGE protocol or with standard NEB conditions to quantify the relative efficiency of restriction digest. The EDGE protocol improved the efficiency of *EcoP15I* cleavage by ~6.4-fold relative to standard NEB conditions ($p = 0.0003$).

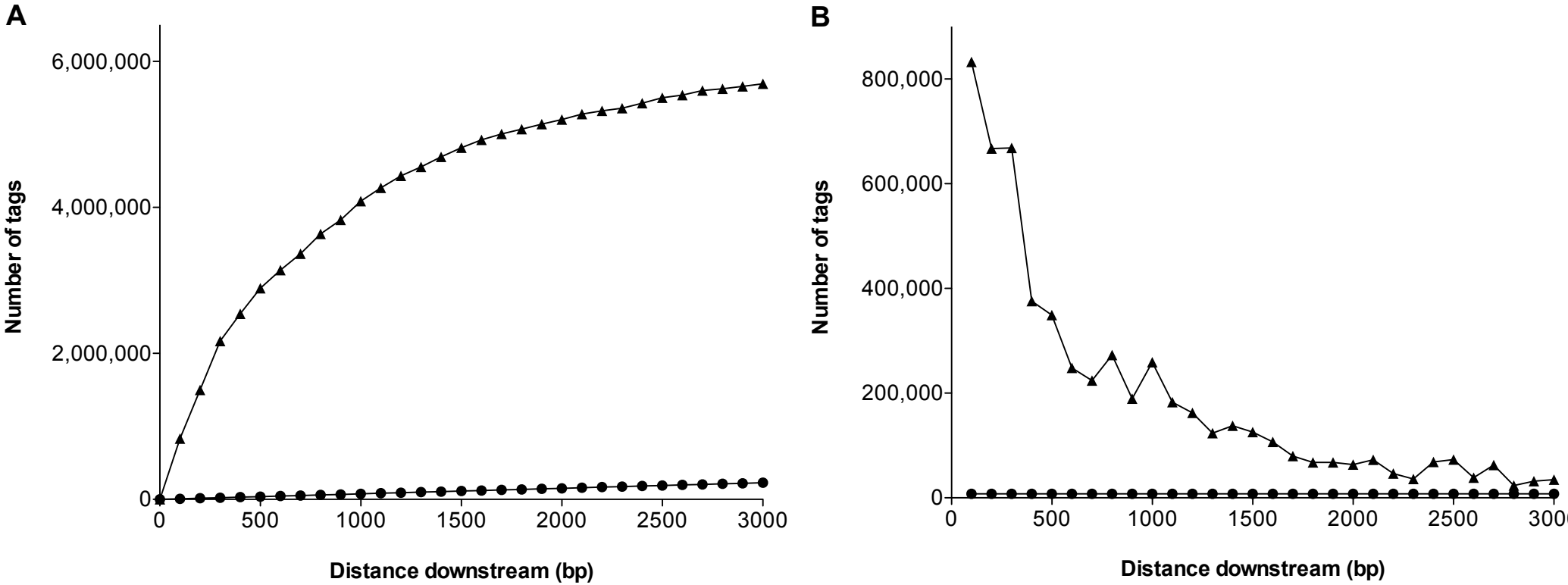

Supplementary Figure 8. Significant enrichment of cheetah EDGE tags downstream of *F. catus* Ensembl transcripts. Representative data from one cheetah EDGE library showing the enrichment of EDGE tags in the three-kilobase region immediately downstream of annotated *F. catus* Ensembl transcripts. (A) shows the increasing number of EDGE tags as horse transcripts are artificially extended in the 3'-direction, while (B) shows the number of EDGE tags that align within each 100 bp interval.

- Frequency of tags observed
- Expected frequency of tags if all "non-exonic" tags mapped randomly across the intergenic space

Supplementary Table 1. PANTHER functional enrichment analysis.

Functional classification	Ontology	Expression in mutant tissue	P-value (neonate dermis)	P-value (spleen)
Receptor activity	Molecular function	Up	2.01E-03	1.05E-05
Response to interferon-gamma	Biological process	Down	7.91E-03	1.52E-03
Signal transduction	Biological process	Up	3.14E-03	4.05E-03
Cell communication	Biological process	Up	6.26E-03	9.53E-03

Statistically over-represented PANTHER functional classification categories within the differentially expressed genes in mouse neonate dermis (327 genes) and spleen (945 genes) were determined by using a binomial statistic tool described in Cho & Campbell (2000). Functional classification categories that were shared between both tissues are shown (p-value < 0.01). At least three genes were required for each category and genes that were detected by EDGE were used as the reference for each tissue.

Supplementary Table 2. Downregulated genes in *Mc1r*$^{e/e}$ neonate dermis have known or predicted functions in innate immunity.

Gene	Average TPM[a]		Fold difference[b]	Function
	Wild type	Mutant		
Ifit1	6.8	0.06	-113.3	interferon-induced protein with tetratricopeptide repeats 1
Oas2	1.2	0	-∞	induced by interferons and uses adenosine triphosphate in 2'-specific nucleotidyl transfer reactions to synthesize 2',5'-oligoadenylates, which then activate latent RNase L and results in viral RNA degradation and the inhibition of viral replication
Oasl2	1.9	0.08	-23.8	2'-5' oligoadenylate synthetase-like 2
Zbp1	10.6	1.0	-10.6	Pattern recognition receptor that mediates IFNalpha/beta responses to cytosolic DNA in mice.
Usp18	3.0	0.4	-7.5	Removes ubiquitin adducts from a broad range of protein substrates. Identified in a screen for interferon-stimulated genes.
Ccdc86	24.0	7.4	-3.2	identified as a novel immediate-early cytokine-responsive gene induced in a hematopoietic cell line by interleukin 3
Gm12250	0.7	0.06	-11.7	interferon-gamma-inducible p47 GTPase. Plays a role in the intracellular resistance to Chlamydia trichomatis.
Iigp1	0.7	0.02	-35	interferon inducible GTPase 1, strongly induced transcriptionally by interferons and implicated in cell-autonomous resistance to intracellular pathogens.

[a] Average of five *Mc1r*$^{+/+}$ and six *Mc1r*$^{e/e}$ EDGE libraries.
[b] Relative to wild type.

Supplementary Table 3. Downregulated genes in *Mc1r*$^{e/e}$ spleen have known or predicted functions in innate immunity.

Gene	Average TPM[a]		Fold difference[b]	Function
	Wild type	Mutant		
Oas2	26.5	4.8	-5.5	induced by interferons and uses adenosine triphosphate in 2'-specific nucleotidyl transfer reactions to synthesize 2',5'-oligoadenylates, which then activate latent RNase L and results in viral RNA degradation and the inhibition of viral replication.
Oasl1	12.4	1.4	-8.6	2'-5' oligoadenylate synthetase-like 1.
Iigp1	50.6	12.3	-4.1	interferon inducible GTPase 1, strongly induced transcriptionally by interferons and implicated in cell-autonomous resistance to intracellular pathogens.
Irgm1	18.1	4.6	-3.9	IFN-gamma inducible; involved in host resistance against intracellular pathogens.
Gbp2	50.3	13.4	-3.8	Guanylate binding protein upregulated during bacteria and protozoan infection.
Gbp4	23.2	8.4	-2.8	Guanylate binding protein upregulated during bacteria and protozoan infection.
Gbp5	7.4	3.1	-2.4	Guanylate binding protein upregulated during bacteria and protozoan infection.
Irf1	796	175	-4.5	Interferon regulatory factor. Stimulates expression of interferon-inducible genes. Enhances TLR-dependent gene induction in IFN-gamma treated cells.
Irf3	215	51.5	-4.2	Induces type I IFN and cytokines upon virus infection, TLR stimulation and cytosolic DNA stimulation.
Irf9	313	124	-2.5	Binds to STAT1 and STAT2 to form ISGF3 and stimulates type I IFN-inducible genes.
Aim2	21.4	10.2	-2.1	Recognizes cytosolic DNA from bacteria and viruses and induces the formation of a capase-1-activating inflammasome.
Trim21	19.3	6.8	-2.8	TRIM21 is significantly induced and interacts with IRF3 during virus infection and is required for IRF3-mediated antiviral responses.
Trim11	26.6	13.7	-1.9	TRIM11 is involved in the endogenous restriction of retroviruses
Trim3	4.3	1.2	-3.6	Members of TRIM family of E3 ligases have been shown to exhibit antiviral

Trim3	4.3	1.2	-3.6	Members of TRIM family of E3 ligases have been shown to exhibit antiviral activities.
Trim39	75.3	23.1	-3.3	Members of TRIM family of E3 ligases have been shown to exhibit antiviral activities.
Jak1	108.6	22.5	-4.8	Protein-tyrosine kinase that is required for IFN-alpha, -beta and -gamma signal transduction pathways.
Tyk2	24.9	6.1	-4.1	Protein-tyrosine kinase required for interferon signal transduction. Impaired type I and II interferon signaling in *Tyk2*$^{-/-}$ mice.

[a] Average of five *Mc1r*$^{+/+}$ and five *Mc1r*$^{e/e}$ EDGE libraries.
[b] Relative to wild type.

Supplementary Table 4. Comparison of EDGE and RNA-Seq using incomplete reference transcriptome.

	EDGE		RNA-Seq	
Fastq reads	11,826,345		16,672,771	
Mouse RefSeq transcriptome[†]	Complete	Incomplete	Complete	Incomplete
Correctly assigned to gene	9,987,929[A]	3,410,058[B] (B/A = 34.1%)	10,666,566[A]	3,446,658[B] (B/A = 32.3%)
Incorrectly assigned to gene[††]		302,661[C] (C/B = 8.9%)		303,960[C] (C/B = 8.8%)

[†] The existing mouse RefSeq transcriptome (referred to as "complete") and a simulated incomplete transcriptome (referred to as "incomplete) were used to align fastq reads from EDGE and RNA-Seq libraries from a mouse neonatal dermis sample.
[††] Reads that could have arisen from multiple locations in the full transcriptome and were incorrectly assigned to genes in the incomplete reference.